International Journal of Thermophysics, Vol. 22, No. 4, 2001

Mathematical Models for Pulse-Heating Experiments[1]

J. Spišiak,[2] F. Righini,[3,4] and G. C. Bussolino[3]

Accurate measurements of thermophysical properties at high temperatures (above 1000 K) have been obtained with millisecond pulse-heating techniques using tubular specimens with a blackbody hole. In the recent trend toward applications, simpler specimens in the form of rods or strips have been used, with simultaneous measurement of the normal spectral emissivity using either laser polarimetry or integrating sphere reflectometry. In these experiments the estimation of the heat capacity and of the hemispherical total emissivity is based on various computational methods that were derived assuming that the temperature was uniform in the central part of the specimen (long thin-rod approximation). The validity of this approach when using specimens with large cross sections (rods, strips) and when measuring temperature on the specimen surface must be verified. The application of the long thin-rod approximation to pulse-heating experiments is reconsidered, and an analytical solution of the heat equation that takes into account the temperature dependence of thermophysical properties is presented. A numerical model that takes into account the temperature variations across the specimen has been developed. This model can be used in simulated experiments to assess the magnitude of specific phenomena due to the temperature gradient inside the specimen, in relation to the specimen geometry and to the specific thermophysical properties of different materials.

KEY WORDS: high temperature; long thin-rod approximation; modeling; pulse heating.

1. INTRODUCTION

In the last thirty years pulse-heating techniques have become accepted methods for the accurate measurement of several thermophysical properties of electrical conductors in the high temperature range [1, 2]. The most

[1] Paper presented at the Fourteenth Symposium on Thermophysical Properties, June 25–30, 2000, Boulder, Colorado, U.S.A.

[2] SAV Institute of Physics, Dubravska cesta 9, 842 28 Bratislava, Slovakia.

[3] CNR Istituto di Metrologia "G. Colonnetti," strada delle Cacce 73, I-10135 Torino, Italy.

[4] To whom correspondence should be addressed. E-mail: f.righini@imgc.to.cnr.it

0195-928X/01/0700-1241$19.50/0

accurate results have been obtained in the characterization of reference materials, using tubular specimens with a blackbody hole [3]; in these cases the temperature is measured with a high-speed pyrometer focussed inside a blackbody machined in the tubular specimen. The blackbody configuration provides true temperature measurement conditions, with the radiation emitted by the blackbody being related to the integral of the longitudinal temperature distribution of the inner part of the tubular specimen. The emissivity of the realized blackbody is generally high (>0.97), but there is uncertainty associated with the limited knowledge of the wall emissivity, surface conditions, and geometrical limitations.

The trend of pulse-heating techniques in recent years has been toward applications oriented activities. Specimens with blackbody holes are difficult to machine, and often materials are not available in tubular form. Two different methods have been developed for direct measurement of the normal spectral emissivity of the specimen surface in pulse-heating conditions. The National Institute of Standards and Technology (NIST, Gaithersburg, Maryland, U.S.A.) and Containerless Research Inc. (CRI, Chicago, Illinois, U.S.A.) have jointly applied laser polarimetry [4]. This technique uses rod specimens and measures directly the normal spectral emissivity of the specimen surface by analyzing the polarization state of the radiation reflected by the specimen surface during the pulse experiment. The technique has been developed for measurements in the solid phase and has been extended to measurements in the liquid state using wire specimens [5, 6]. Alternatively, the Istituto di Metrologia "Gustavo Colonnetti" (IMGC, Torino, Italy) has developed an integrating sphere reflectometric technique to measure the normal spectral emissivity of a strip specimen during pulse heating with measurements performed in the solid phase including the melting plateau [7, 8].

Measurements of the heat capacity and of the electrical resistivity of molybdenum in the temperature range 2000 to 2800 K performed at the NIST [9] have indicated the validity of the laser polarimetry technique, providing results of similar accuracy as those obtained using tubular specimens with a blackbody configuration. Similarly, experimental results of the heat capacity and of the electrical resistivity of niobium in the temperature range 1400 to 2700 K performed at the IMGC [10] on strip specimens with integrating sphere reflectometry provided results of comparable accuracy with respect to measurements performed earlier using a blackbody configuration.

For both techniques (laser polarimetry and integrating sphere reflectometry) the main difference with respect to measurements in a blackbody configuration is that the temperature of a small portion of the specimen surface is assumed to be representative of the entire specimen. For very

accurate experimental work, we consider in this paper the limitations of this assumption, by developing a mathematical model that describes a long thick specimen, with a temperature gradient along its cross section. The mathematical formulation used in the computation of thermophysical properties from experimental quantities in pulse-heating experiments has generally accepted a mathematical simplification known as the "long thin rod" approximation. This simplification implies that the specimen is sufficiently thin to have no significant temperature gradient along its cross section. In examining this approximation, an analytical solution is presented that takes into account the temperature dependence of thermophysical properties.

2. FORMULATION OF THE PROBLEM

Two specimen geometries are considered: a rod (Fig. 1) and a strip (Fig. 2), representative, respectively, of laser polarimetry and of integrating sphere reflectometry experiments. The specimens are considered to be geometrically perfect (no variations of cross section) and with a normal spectral emissivity identical at any surface point. With these assumptions, simultaneous measurement at the same wavelength of the normal spectral

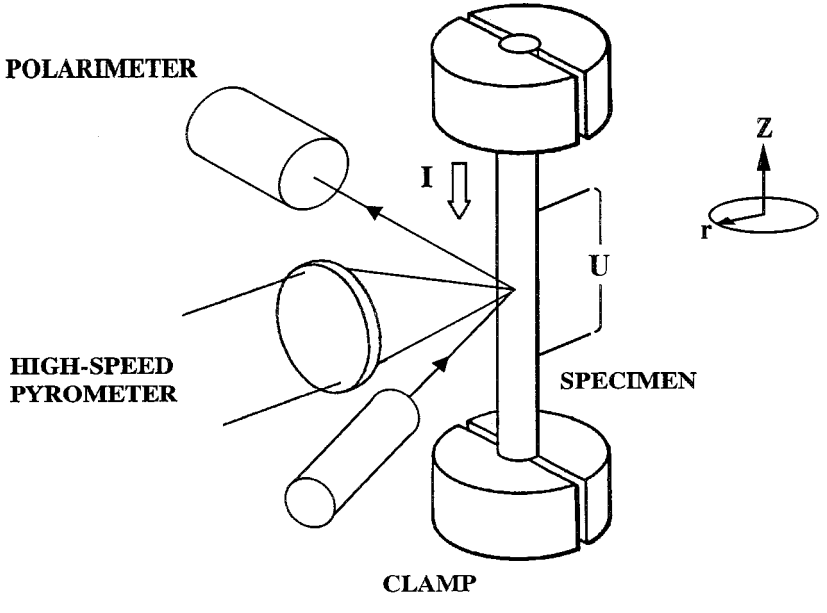

Fig. 1. Schematic of the cylindrical specimen used for pulse-heating experiments with laser polarimetry.

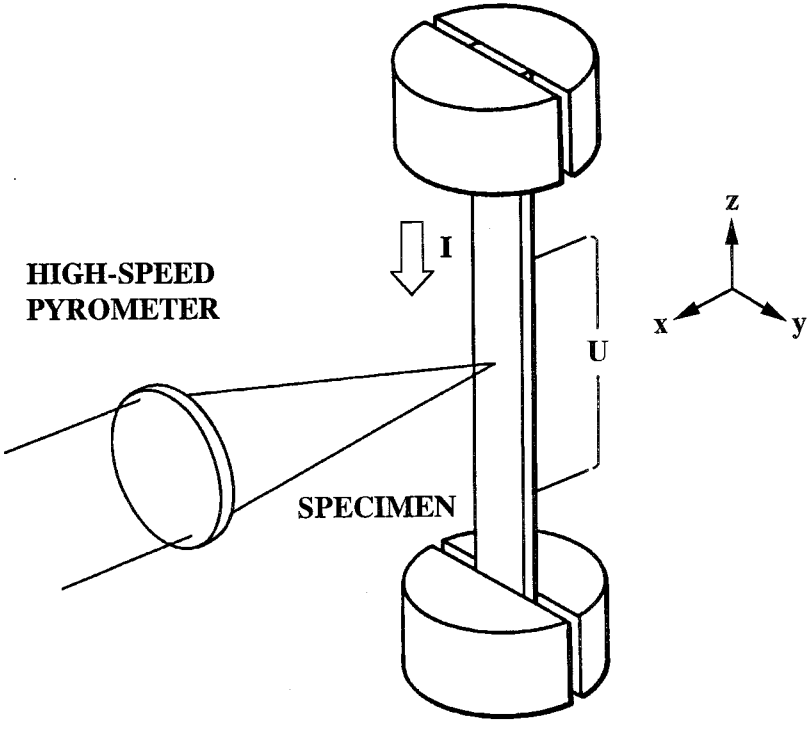

Fig. 2. Schematic of the strip specimen used in integrating sphere reflectometry under pulse-heating conditions.

emissivity and of the radiance temperature of the surface can provide information on the true temperature of the specimen.

Heat diffusion in electrical conductors is described by the partial differential equation:

$$\delta C_p \frac{\partial T}{\partial t} = \nabla \cdot \lambda \nabla T + \mu \mathbf{i} \cdot \nabla T + \rho \mathbf{i}^2 \tag{1}$$

where each term of Eq. (1) describes a phenomenon taking place in the specimen on the passage of an electrical current. The symbols denote the following properties: δ, density; C_p, heat capacity at constant pressure; T, temperature; ∇T, temperature gradient; λ, thermal conductivity; μ, Thomson coefficient; $\mathbf{i}$, electrical current density; and ρ, electrical resistivity. The derivation of the heat equation for metals and semiconductors on the basis of nonequilibrium thermodynamics can be found in the literature [11]. In pulse-heating experiments with a sufficiently fast heating rate,

temperature profiles with a flat central part $[\mathrm{d}T(x, y, z, t)/\mathrm{d}z = 0]$ are obtained. For this central portion of the specimen, one can write a simplified version of Eq. (1) that takes into account the radial temperature distribution in a cylindrical coordinate system where the z-axis is the center of the rod-shaped specimen (Fig. 1),

$$\delta C_p \frac{\partial T(r, t)}{\partial t} = \frac{1}{r} \frac{\partial}{\partial r} \left(r\lambda \frac{\partial T(r, t)}{\partial r} \right) + \rho [i(r, t)]^2 \tag{2a}$$

or for a slab (or a wide strip) where the x-axis is perpendicular to the surface (Fig. 2)

$$\delta C_p \frac{\partial T(x, t)}{\partial t} = \frac{\partial}{\partial x} \left(\lambda \frac{\partial T(x, t)}{\partial x} \right) + \rho [i(x, t)]^2 \tag{2b}$$

The Thomson heat term $\mu \mathbf{i} \cdot \nabla T$ in these cases is zero because the direction of the current density $\mathbf{i}$ and of the temperature gradient ∇T are perpendicular to each other.

The Eqs. (2) are a mathematical model for a long and thick specimen because they take into consideration the temperature gradient in the cross section of the specimen, which is a physical consequence of the radiation losses from the specimen surface. The possibility of practical use of Eqs. (2) for numerical simulations of the experiments is limited, because the current distribution in the specimen is unknown. On the other hand the spatial distribution of the input power can be computed from the voltage drop measured in the central part of the specimen. Using the simple Ohm's law we have to be aware that we are neglecting

- the skin effect when the current is switched on,
- other phenomena which may also contribute to the electric field.

The influence of a nonuniform electric field in pulse-heating experiments was studied by Lohöfer [12], who pointed out that the transient skin effect has a limited influence because of its short duration. Depending on the geometrical configuration of the experimental setup, the skin effect vanishes a few milliseconds after the current is switched on. In a subsecond experiment, during this transient of millisecond duration, the specimen is still at very low temperatures where no pyrometric measurements are generally performed. Consequently the skin effect taking place at the beginning of the experiment can be neglected.

The relation between the electric field and the current density for quasi-stationary processes (like the subsecond experiments, where the

specimen is heated by a dc current pulse lasting several hundred milliseconds) is governed by the equation

$$\mathbf{E} = \frac{1}{e} \nabla \xi - S \nabla T + \rho \mathbf{i} \tag{3}$$

where ξ is the chemical potential; e, the electrical charge of one electron; and S, the Seebeck coefficient. In pulse-heating experiments large currents (thousands of amps) are applied and, therefore, the last term in Eq. (3) is dominant while the remaining terms can be neglected. In a scalar representation,

$$E(r, t) \cong \rho i(r, t) \tag{4}$$

By substituting Eq. (4) into Eqs. (2) we obtain relations that are suitable for the computation of the temperature profiles inside the specimen. For a rod-shaped specimen

$$\delta C_p \frac{\partial T(r, t)}{\partial t} = \frac{1}{r} \frac{\partial}{\partial r} \left(r\lambda \frac{\partial T(r, t)}{\partial r} \right) + \frac{[E(r, t)]^2}{\rho} \tag{5}$$

and a similar expression holds for a slab (or a wide strip). During the free cooling period the power is switched off and the last term in Eq. (5) is equal to zero.

This partial differential equation must be solved with the appropriate initial and boundary conditions. At the beginning of the experiment we assume that the specimen is in temperature equilibrium with its surroundings at ambient temperature T_a. The initial condition for the heating period is therefore $T_{\text{initial}}(r, t) = T_a$. The initial condition for the cooling period is obtained from the last temperature distribution during the heating period. In this mathematical model the boundary conditions are quite simple because heat is propagating only in one direction (r for rod and x for slab) towards the specimen surface. At the surface the heat balance is defined by the Fourier and Stefan–Boltzmann laws:

$$-\lambda \frac{\partial T_{\text{surface}}}{\partial x} = \varepsilon_{ht} \sigma (T^4_{\text{surface}} - T^2_a) \tag{6}$$

where ε_{ht} is the hemispherical total emissivity and σ is the Stefan–Boltzmann constant. An additional boundary condition can be written on account of the symmetry of the model. This does not improve the result but it saves some computation time. At the center of the specimen (in the rod case $r = 0$ and in the slab case $x = 0$), the temperature profiles maintain their symmetry

$\partial T/\partial r|_{r=0}=0$ and $\partial T/\partial x|_{x=0}=0$, respectively. It can be easily demonstrated that the classical relations used for the computation of heat capacity and hemispherical total emissivity in subsecond pulse-heating experiments [1] are derived from a simplified version of the more general case presented earlier. We can consider a simplified model (generally known as a long thin rod approximation) in which the entire volume of the central part of the specimen is uniformly heated and cooled. This simplification means that the cross-sectional thermal conduction is neglected, and the radiation heat losses at the surface are included in the heat equation in order to maintain the power balance of the central part of the rapidly heated specimen. By integrating Eqs. (2) over the volume and adding the radiation loss term, we get

$$mC_p\left(\frac{dT}{dt}\right)_h = P-\varepsilon_{ht}\sigma A(T^4-T_a^4) \tag{7}$$

where m and A are the mass and the radiating surface area of the central portion of the specimen while P is the input power. During cooling the current is switched off ($P=0$)

$$mC_p\left(\frac{dT}{dt}\right)_c = -\varepsilon_{ht}\sigma A(T^4-T_a^4) \tag{8}$$

Eqs. (7) and (8) are the power balance relations usually considered for the computation of thermophysical properties in pulse-heating experiments using a long thin rod approximation [1].

3. SIMULATION OF PULSE-HEATING EXPERIMENTS

Subsecond pulse-heating experiments are performed in a wide temperature range (up to several thousand kelvins). The thermophysical properties of the specimen change considerably with temperature in such a wide range, and this variation must be considered in any numerical simulation. The temperature dependence is generally represented by means of polynomial functions, e.g.,

3.1. Long Thin-Rod Approximation

If we apply the temperature dependence of properties C_p and ε_{ht} to Eq. (7) and use as input power the experimentally measured quantities voltage drop U and current I passing through the specimen, we obtain

$$UI-\varepsilon_{ht}(T)\,A\sigma(T^4-T_a^4)=mC_p(T)\frac{dT}{dt} \tag{10}$$

If the input power is expressed as

- $P = P(t)$ function of time t, then the simulation according to Eq. (10) can be performed via a Runge–Kutta algorithm,
- $P = P(T)$ function of temperature T, then even an analytical solution of Eq. (10) is possible.

Let us assume that, besides thermophysical properties, also the input power $P = P(T)$ can be represented as a polynomial in temperature. In this case we obtain a first-order ordinary differential equation,

$$\frac{dt}{dT} = \frac{mC_p(T)}{P(T) - \varepsilon_{ht}(T)\,\sigma A(T^4 - T_a^4)} \tag{11}$$

that can be integrated to obtain

$$t = t_{in} + \int_{T_{in}}^{T} \frac{mC_p(\vartheta)\,d\vartheta}{P(\vartheta) - \varepsilon_{ht}(T)\,\sigma A(\vartheta^4 - \vartheta_a^4)} \tag{12}$$

This equation can be easily solved either numerically by means of a Romberg integration [13] or analytically, with the initial condition that at time t_{in} the temperature is T_{in}.

The analytical solution of Eq. (12) can be computed by dividing the subintegral function into rational fractions. The advantage of the analytical solution of the integral is that the computation is very fast with high numerical precision (better than 10^{-8} K). The method is especially suitable for the simulation of the cooling phase on account of zero input power ($P = 0$) where the initial condition is the highest temperature reached in the heating period.

3.2. Long Thick-Rod Approximation

Equation (5), together with the surface condition Eq. (6), is a nonlinear parabolic heat equation. These equations with an initial condition can be solved numerically by means of an explicit finite difference method. This approach uses a forward finite difference for the time derivative and a central finite difference for the diffusive term. Let Δt and Δx denote discrete steps in time and space, respectively. The temperature $T_j^n = T(j\,\Delta x, n\,\Delta t)$ is now evaluated only in this mesh that consists of equidistant points. The advantage of the explicit method is that the temperature at time $j+1$ is computed according to the properties and temperatures at time j

$$\delta C_p \frac{T_j^{n+1} - T_j^n}{\Delta t} = \frac{\lambda_{j+1/2}(T_{j+1}^n - T_j^n) - \lambda_{j-1/2}(T_j^n - T_{j-1}^n)}{\Delta x^2} + \frac{E^2}{\rho} \tag{13}$$

or

$$T_j^{n+1} = [1 - \alpha(\lambda_{j+1/2} - \lambda_{j-1/2})]\, T_j^n + \alpha\lambda_{j+1/2} T_{j+1}^n + \alpha\lambda_{j-1/2} T_{j-1}^n + \frac{E^2\, \Delta t}{\rho\, \delta C_p} \tag{14}$$

where $\alpha = \Delta t/\delta C_p\, \Delta x^2$, and $\lambda_{j+1/2}$ or $\lambda_{j-1/2}$ is the average thermal conductivity between the mesh points $j+1$, j and j, $j-1$, defined as

$$\lambda_{j+1/2} = 0.5[\lambda(T_{j+1}^n) + \lambda(T_j^n)], \qquad \lambda_{j-1/2} = 0.5[\lambda(T_j^n) + \lambda(T_{j-1}^n)] \tag{15}$$

The numerical system, Eq. (14), is stable if all terms on the right-hand side are non-negative. It can be easily proven that if discretization parameters satisfy the following inequality,

$$\Delta t \leqslant \min_j \left(\frac{\Delta x^2\, C_{pj} \delta_j}{2\lambda_{j+1/2}} \right) \tag{16}$$

then the computation is stable. A similar inequality can be written also for the cylindrical coordinate system. The boundary condition (Eq. 6) is used to compute the temperature on the surface while for the remaining points, Eq. (14) is applied. The precision of computed temperature profiles using a mesh of 200 points is better then 10^{-4} K.

4. CONCLUSIONS

The application of the long thin-rod approximation to pulse-heating experiments has been reconsidered, and an analytical solution that takes into account the temperature dependence of the thermophysical properties has been presented. Extensive software programs have been developed for the numerical simulation of pulse-heating experiments of subsecond duration. The mathematical models are based both on a long thin rod and also on a long thick rod (or a long thick strip). This second and more general model considers the temperature gradients in the specimen cross section. The application of the more general mathematical model to a tungsten rod specimen with a diameter of 3.2 mm is presented in Fig. 3 by plotting the temperature profiles inside the rod as a function of temperature during a pulse-heating experiment where the melting point is reached in 0.42 s. The temperature profile is well within experimental uncertainties in temperature measurements up to 2000 K, but becomes significant above this temperature. The work is continuing with a systematic application of the developed software to different materials and different specimen geometries, to evaluate

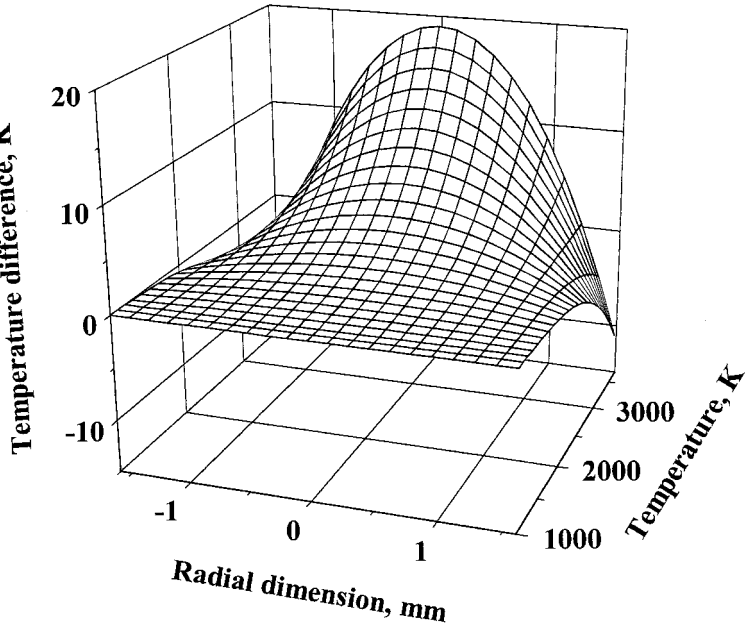

Fig. 3. Simulated temperature profile inside a tungsten rod of 3.2 mm diameter taken to its melting point in a pulse-heating experiment of 0.42 s duration.

potential problems in pulse-heating experiments when using specimens with large cross sections. The influence of the direct measurement of the radiance temperature on the specimen surface with simultaneous determination of the normal spectral emissivity via laser polarimetry or integrating sphere reflectometry on the accuracy of thermophysical properties will be investigated, using realistic experimental conditions.

ACKNOWLEDGMENT

One of the authors (JS) gratefully acknowledges the support received from Slovak Grant Agency (VEGA) under Contract No. 2/1125/21.

REFERENCES

1. A. Cezairliyan, in *Compendium of Thermophysical Property Measurement Methods*, Vol. 1, K. D. Magliç, A. Cezairliyan, and V. E. Peletskii, eds. (Plenum, New York, 1984), pp. 643–668.
2. A. Cezairliyan, in *Compendium of Thermophysical Property Measurement Methods*, Vol. 2, K. D. Magliç, A. Cezairliyan, and V. E. Peletskii, eds. (Plenum, New York, 1992), pp. 483–517.

3. F. Righini, G. C. Bussolino, and J. Spišiak, *Thermochimica Acta* **347**:93 (2000).
4. A. Cezairliyan, S. Krishnan, and J. L. McClure, *Int. J. Thermophys.* **17**:1455 (1996).
5. A. Seifter, F. Sachsenhofer, S. Krishnan, and G. Pottlacher, *Int. J. Thermophys.* (in press).
6. K. Boboridis, *Int. J. Thermophys.* (in press).
7. F. Righini, G. C. Bussolino, and A. Rosso, in *Proceedings of TEMPMEKO'96*, P. Marcarino, ed. (Levrotto Bella, Torino, Italy, 1997), pp. 489–492.
8. F. Righini, J. Spišiak, and G. C. Bussolino, *Int. J. Thermophys.* **20**:1095 (1999).
9. A. Cezairliyan, S. Krishnan, D. Basak, and J. L. McClure, *Int. J. Thermophys.* **19**:1267 (1998).
10. F. Righini, J. Spišiak, G. C. Bussolino, and M. Gualano, *Int. J. Thermophys.* **20**:1107 (1999).
11. Š. BArta, *Int. J. Heat Mass Transfer*. **39**:3531 (1996).
12. G. Lohöfer, *Int. J. of Thermophys.* **14**:471 (1993).
13. W. H. Press, S. A. Teukolsky, W. T. Vetterling, and B. P. Flannery, in *Numerical Recipes in FORTRAN: the Art of Scientific Computing*, 2nd ed. (Cambridge University Press, 1992), pp. 483–517.